BIOCHEMISTRY
including biophysical chemistry & molecular biology

Article

pubs.acs.org/biochemistry

Antimicrobial Peptide Lactoferricin B-Induced Rapid Leakage of Internal Contents from Single Giant Unilamellar Vesicles

Md. Moniruzzaman,[†] Jahangir Md. Alam,[‡] Hideo Dohra,[§] and Masahito Yamazaki*[,†,‡,∥]

[†]Integrated Bioscience Section, Graduate School of Science and Technology, [‡]Nanomaterials Research Division, Research Institute of Electronics, [§]Instrumental Research Support Office, Research Institute of Green Science and Technology, and [∥]Department of Physics, Faculty of Science, Shizuoka University, Shizuoka 422-8529, Japan

ABSTRACT: Enzymatic digestion of bovine lactoferrin generates lactoferricin B (Lfcin B), a 25-mer peptide with strong antimicrobial activity of unknown mechanism. To elucidate the mechanistic basis of Lfcin B bactericidal activity, we investigated the interaction of Lfcin B with *Escherichia coli* and liposomes of lipid membranes. Lfcin B induced the influx of a membrane-impermeant fluorescent probe, SYTOX green, from the outside of *E. coli* into its cytoplasm. Lfcin B induced gradual leakage of calcein from large unilamellar vesicles (LUVs) of dioleoylphosphatidylglycerol (DOPG)/dioleoylphosphatidylcholine (DOPC) membranes. To clarify the cause of Lfcin B-induced leakage of calcein from the LUVs, we used the single giant unilamellar vesicle (GUV) method to investigate the interaction of Lfcin B with calcein-containing DOPG/DOPC-GUVs. We observed that a rapid leakage of calcein from a GUV started stochastically; statistical analysis provided a rate constant for Lfcin B-induced pore formation, k_p. On the other hand, phase-contrast microscopic images revealed that Lfcin B induced a rapid leakage of sucrose from the single GUVs with concomitant appearance of a spherical GUV of smaller diameter. Because of the very fast leakage, and at the present time resolution of the experiments (33 ms), we could not follow the evolution of pore nor the process of the structural changes of the GUV. Here we used the term "local rupture" to express the rapid leakage of sucrose and determined the rate constant of local rupture, k_L. On the basis of the comparison between k_p and k_L, we concluded that the leakage of calcein from single GUVs occurred as a result of a local rupture in the GUVs and that smaller pores inducing leakage of calcein were not formed before the local rupture. The results of the effect of the surface charge density of lipid membranes and that of salt concentration in buffer on k_p clearly show that k_p increases with an increase in the extent of electrostatic interactions due to the surface charges. Analysis of Lfcin B-induced shape changes indicated that the binding of Lfcin B increased the area of the outer monolayer of GUVs. These results indicate that Lfcin B-induced damage of the plasma membrane of *E. coli* with its concomitant rapid leakage of internal contents is a key factor for the bactericidal activity of LfcinB.

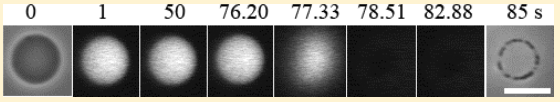

Lactoferrin (LF) is a transferrin-like glycoprotein present in exocrine secretions such as milk.[1,2] LF in milk is hydrolyzed to various peptides by pepsin digestion under acidic conditions (e.g., in mammal stomach); some of the resulting peptides exhibit antimicrobial activity.[3,4] Depending on the species of origin, these peptides are designated lactoferricin B (Lfcin B) (derived from bovine lactoferrin) or lactoferricin H (Lfcin H) (derived from human lactoferrin).[3] Lfcin B and Lfcin H provide a natural defense against a wide range of Gram-negative and Gram-positive bacteria, yeast, and filamentous fungi,[3,5,6] and have antitumor activity and immunomodulatory activities.[1,7,8] Lfcin B is composed of 25 amino acids, with an amino acid sequence of FKCRRWQWR-MKKLGAPSITCVRRAF. Thus, Lfcin B is a highly positively charged peptide, containing five R residues and three K residues.[5] Lfcin B has a disulfide bond, although this bond is not important for bactericidal activity.[5] The three-dimensional structure of Lfcin B in aqueous solution reveals a somewhat distorted antiparallel β-sheet; the molecule is amphipathic, containing a hydrophobic surface (composed of residues F1, C3, W6, W8, P16, I18, and C20) opposite a hydrophilic surface containing the charged residues.[9] This amphipathic structure is reminiscent of other antimicrobial peptides (AMPs).[10−12] Shorter segments of Lfcin B also have antimicrobial activity.[7,13−15] An all-D amino acid derivative of a nonamer core peptide of Lfcin B exhibits the same antibacterial activity as that of natural, all-L Lfcin B.[16,17] This observation suggests that the target of Lfcin B is the lipid membrane region of bacterial and fungal biomembranes. Notably, although Lfcin H (with a length of 47 residues[3]) is almost double the size of Lfcin B, the human peptide (i.e., Lfcin H) also exhibits an amphipathic structure by structural analysis.[18] The antimicrobial activity of Lfcin B is much higher than that of Lfcin H,[3] and therefore the majority of research on Lfcins has employed the bovine homologue.

To date, most studies on the interactions of AMPs with lipid membranes have been performed using a suspension of many large unilamellar vesicle (LUVs) (i.e., the LUV suspension method).[19] Investigation on interaction of lactoferricin with the lipid membrane using the LUV suspension method has revealed that lactoferricin induces leakage of K^+ and H^+.[20−22] In these studies, the average values of the physical parameters of vesicles have been obtained from a large number of vesicles, and thereby much information has been lost. Recently we have

Received: June 1, 2015
Revised: September 12, 2015
Published: September 14, 2015

DOI: 10.1021/acs.biochem.5b00594
Biochemistry 2015, 54, 5802−5814

developed a novel method, the single giant unilamellar vesicle (GUV) method. In this method, we observe and measure the changes in the structure and physical properties of a single GUV with a diameter of ≥10 μm that are induced by interactions of compounds such as peptides and proteins with the lipid membrane as a function of time and spatial coordinates. The same experiment is repeated many times using other single GUVs. Then we combine all the independent experiments and make statistical analysis of the changes in the physical properties of a single GUV over the results of many "single GUVs" to obtain rate constants for the elementary processes underlying the structural changes and functions of GUVs.[19,23] Using this method, we obtained new information on the interaction of a specific AMP (magainin 2) with membrane vesicles. Specifically, during the interaction of magainin 2 with a single GUV encapsulating a fluorescent probe (calcein), a rapid reduction in the fluorescence intensity inside the GUV occurred stochastically. These results indicated that binding of magainin 2 to the GUV induced stochastic pore formation in the GUV membrane, thereby permitting leakage of calcein from the GUV. By analyzing the time course of the fraction of intact (no leakage of fluorescent probe) GUVs among all examined GUVs, we obtained the rate constant of the magainin 2-induced pore formation, k_p, and also the rate constants of membrane permeation (or leakage) through the magainin 2-induced pores, k_{mp}.[24−27] We also investigated the interaction of an antibacterial substance, (−)-epigallocatechin gallate (EGCg), with lipid membranes using the single GUV method. This analysis demonstrated that EGCg induced bursting of the GUVs, through which calcein leakage occurred from the GUV.[28] Recently, another method using GUVs, i.e., the GUV suspension method, was also used for analysis of influx of fluorescent probes from the outside to the inside of GUVs.[29−31] The comparison of the single GUV method and the GUV suspension method is described in our previous perspective and papers.[23,27,39] Hence, the single GUV method and the GUV suspension method can provide a great deal of new information that would not otherwise be obtainable by the conventional LUV suspension method.

In the present report, we elucidated the mechanism of the antimicrobial activity of Lfcin B by investigating the interaction of this AMP with *Escherichia coli* and with liposomes composed of negatively charged dioleoylphosphatidylglycerol (DOPG) and electrically neutral dioleoylphosphatidylcholine (DOPC) mixtures. First we investigated the interaction of Lfcin B with *E. coli*. The results indicated that Lfcin B induced the influx of a membrane-impermeant fluorescent probe, SYTOX green, from the extracellular space into the cytoplasm; these data suggested that Lfcin B's bactericidal activity reflects damage to the *E. coli* plasma membrane. Second, Lfcin B-induced leakage of calcein from LUVs and GUVs of 50 mol %DOPG/50 mol %DOPC (hereafter PG/PC (1/1)) was investigated to permit direct assessment of membrane damage by Lfcin B. Third, to elucidate the mechanism of the Lfcin B-induced calcein leakage, we investigated peptide-induced structural changes in single GUVs. Fourth, we investigated the effects of electrostatic interactions on the Lfcin B-induced calcein leakage using DOPG/DOPC membranes with different DOPG concentration, i.e., 20 mol %DOPG/80 mol %DOPC (hereafter PG/PC (1/4)). On the basis of these results, we discuss the mechanism of the Lfcin B-induced damage to lipid membranes.

MATERIALS AND METHODS

Materials. DOPC and DOPG were purchased from Avanti Polar Lipids Inc. (Alabaster, AL). Calcein was purchased from Dojindo Laboratory (Kumamoto, Japan). SYTOX green and Texas-Red Dextran 70000 (TRD-70k) were purchased from Invitrogen, Inc. (Carlsbad, CA). TRD-70K was used without further purification. Bovine serum albumin (BSA) was purchased from Wako Pure Chemical Industry Ltd. (Osaka, Japan).

Peptide Synthesis and Identification of Peptides. Lfcin B was synthesized by the FastMoc method using a 433A peptide synthesizer (PE Applied Biosystems, Foster City, CA). The sequence of Lfcin B (25-mer) is FKCRRWQWRMKKL-GAPSTICVRRAF with an amide-blocked C terminus. The peptide was cleaved from the resin using trifluoroacetic acid, 1,2-ethanedithiol, and Milli-Q water (9.5/0.25/0.25, volume ratio). Analysis and purification of the peptides were done using reversed phase HPLC, which were described previously.[24−26] The main peak of a HPLC chromatogram of the crude peptides was the reduced Lfcin B (with two sulfhydryl groups) with a mass of 3122.70 Da, and to obtain purified peptides we collected the fraction of main peak, and then lyophilized it. The lyophilized powder was used as the purified peptide. Only one peak was observed in a HPLC chromatogram of the purified peptide, which was the oxidized Lfcin B (i.e., with a disulfide bond) with a mass of 3120.70 Da. The values of mass of the peptides correspond to the molecular masses calculated from the amino acid composition. These results indicate that the reduced Lfcin B was easily oxidized by air. The mass of peptides and identification of the reduced and oxidized Lfcin B were measured using LC−MS analysis as follows.

LC−MS analysis of the sample was performed by a linear ion trap time-of-flight mass spectrometer (LIT−TOF MS), Nano-Frontier eLD (Hitachi High-Technologies Corporation) coupled to a nanoflow HPLC, NanoFrontier nLC (Hitachi High-Technologies Corporation). Two microliters of the sample was trapped and desalted with a C18 monolith trap column (0.05 mm ID × 150 mm long; Hitachi High-Technologies Corporation) and then loaded onto a MonoCap C18 Fast-flow column (0.05 mm ID × 150 mm long; GL Sciences, Inc., Tokyo, Japan) and eluted with a linear gradient from 5 to 100% (v/v) solvent B in 110 min at a flow rate of 200 nL/min. Solvent A was 2% acetonitrile and 0.1% formic acid, and solvent B was 98% acetonitrile and 0.1% formic acid. The eluent was ionized with a nanoelectrospray ionization source equipped with an uncoated SilicaTip (New Objective, Woburn, MA) and analyzed with a LIT−TOF MS. The mass spectrum was obtained in positive ion mode at scan mass range m/z 200−2000 and analyzed by the NanoFrontier eLD Data Processing software (Hitachi High-Technologies Corporation).

Lfcin B concentrations in buffer were determined by absorbance using the molar extinction coefficient of Trp at 280 nm (i.e., 5500 M^{-1} cm^{-1}).

Measurement of Minimum Inhibitory Concentration (MIC). We measured the MIC of Lfcin B against *E. coli* (JM-109) using the standard method.[32,33] Briefly, a suspension of *E. coli* in Nutrient Broth medium was mixed with various concentrations of Lfcin B solution in the individual wells of a 96-well plate. The final density of bacteria in the wells was 10^5 CFU (colony forming unit)/mL, and the final peptide concentration in the wells ranged from 0.12 to 8.0 μM. After incubation at 37 °C for 18−20 h, the absorbance at 600 nm

DOI: 10.1021/acs.biochem.5b00594
Biochemistry 2015, 54, 5802−5814

(Abs (600)) was measured using a microplate reader (Infinite M200, TECAN, Grödig, Austria). The MIC was defined as the lowest concentration of peptide at which there was no change in Abs (600).

Lfcin B-Induced Influx of SYTOX Green into *E. coli*. A suspension of *E. coli* (JM-109) in Nutrient Broth medium was centrifuged (350*g*, 10 min), and the pellet was resuspended in buffer A (10 mM PIPES, pH 7.0, 150 mM NaCl, and 1.0 mM EGTA). Aliquots of this *E. coli* suspension were mixed with SYTOX green in DMSO solution, and then mixed with various concentrations of Lfcin B solution, yielding mixtures with final bacterial densities of ~10^6 CFU/mL, final SYTOX green concentrations of 5.0 μM, final Lfcin B concentrations of 0−50 μM, and final DMSO concentrations of 0.25% (v/v) (for the experiments of Lfcin B concentration dependence shown in Figure 1A). Immediately after the mixing, we started to measure the fluorescence intensity of the mixture. In separate experiments, aliquots of *E. coli* suspensions at various densities were mixed with SYTOX green in DMSO solution and then mixed with a given concentration of Lfcin B solution, yielding mixtures with final Lfcin B concentrations of 20 μM and final SYTOX green concentrations of 5.0 μM (for the experiments of the dependence of *E. coli* density shown in Figure 1B). Immediately after the mixing, we started to measure the fluorescence intensity of the mixture. The time courses of fluorescence intensities of these suspensions were measured using a Hitachi F7000 spectrofluorometer (Hitachi, Tokyo, Japan). Fluorescence intensities of samples were measured at the excitation wavelength 480 nm, the emission wavelength 550 nm, and the excitation and emission band-pass 1.5 nm. The temperature of the cell was held at 25 °C with a water bath circulator (Cool-Bit circulator, ACE-05AN, KELK (old name: Komatsu), Ltd., Tokyo, Japan). For 100% permeabilization of *E. coli*, 1.5 mL of the same suspension of *E. coli* without Lfcin B was pelleted by centrifugation (350*g*, 10 min), and the pellet was resuspended in 2.0 mL 70% 2-propanol and allowed to stand at room temperature for 2.0 h. This *E. coli* suspension was pelleted by centrifugation (14000*g*, 20 min, 20 °C) and resuspended in 2.0 mL of buffer A. The fluorescence intensity of this suspension under the above conditions was taken as 100% SYTOX influx. The fluorescence intensity of the suspension in the absence of Lfcin B at t = 0 was taken as 0% SYTOX influx.

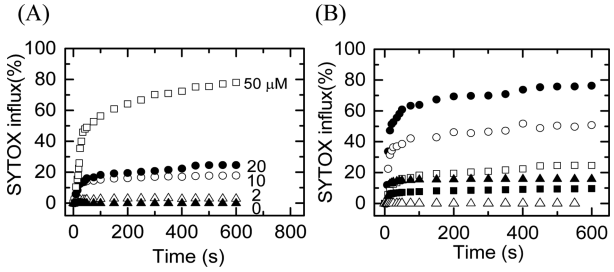

Figure 1. Time course of influx of SYTOX green into cytoplasm of *E. coli*. (A) Time course of fluorescence intensity of SYTOX green during the interaction of various concentrations of Lfcin B with *E. coli* suspension at 25 °C. Lfcin B concentration is described at the right of each curve. Bacteria density was 1.0 × 10^6 CFU/mL. (B) Time course of fluorescence intensity of SYTOX green during the interaction of 20 μM Lfcin B with suspensions of various density of *E. coli* at 25 °C. Final bacterial densities were 1.0 × 10^5 (●), 1.4 × 10^5 (○), 1.0 × 10^6 (□), 1.0 × 10^7 (▲), 1.5 × 10^7 (■), and 0.0 CFU/mL (Δ).

Interaction of Lfcin B with PG/PC (1/1)-LUV Suspension. PG/PC (1/1)-LUVs were prepared by the extrusion method.[24] First we prepared multilamellar vesicles (MLVs) of PG/PC (1/1) containing calcein solution. For this purpose, 1.0 mL of 70 mM calcein in Milli-Q (pH 7.0; adjusted with NaOH) was added to dry lipid film of PG/PC (1/1), and the suspension was vortexed several times for ~20 s at room temperature. Next, the MLV suspension was subjected to five cycles of freezing in liquid N_2 for 1.0 min, followed by warming to room temperature for 25−30 min (freeze−thawing). The resulting solution was extruded through a 200 nm-pore-size Nuclepore membrane using LF-1 LiposoFast apparatus (Avestin, Ottawa, Canada) until the solution became transparent. To remove the untrapped calcein, the LUV suspension was passed through a Sephadex G-75 column equilibrated in buffer A. A Hitachi F7000 spectrofluorometer was used for fluorescence measurement. Fluorescence intensities of samples were measured at the excitation wavelength 490 nm, the emission wavelength 520 nm, and the excitation and emission band-pass 1.5 nm. The temperature of the cell was held at 25 °C with a water bath circulator (Cool-Bit circulator). The fluorescence intensity of the PG/PC (1/1)-LUV suspension in the absence of Lfcin B and that in the presence of 0.6% (v/v) Triton X-100 were taken as 0% and 100% leakage, respectively. The lipid concentrations in the sample were determined by the Bartlett method.[34]

Experiments Using the Single GUV Method. PG/PC-GUVs were prepared by the natural swelling method.[24] Milli-Q water (20 μL) was added into a dry lipid film in a glass vial (volume: 5 mL), and the mixture was incubated at ~45 °C for ~7 min (prehydration) and then incubated with 1.0 mL of buffer A containing 0.10 M sucrose for 2−3 h at 37 °C. To obtain a purified GUV suspension, smaller vesicles and untrapped fluorescent probes were removed using the membrane filtering method.[35] Briefly, the suspension was centrifuged (14000*g*, 20 min, 20 °C); the resulting supernatant was filtered through a Nuclepore membrane with 10-μm diameter pores (Whatman, GE Healthcare, UK, Ltd., Buckinghamshire, UK) in buffer A containing 0.10 M glucose for 1.0 h at a flow rate of 1.0 mL/min at room temperature (20−25 °C); the retained suspension (i.e., that which did not pass through the filter) was collected and used as the purified GUV suspension in the following experiments. To prepare GUVs containing water-soluble fluorescent probe, calcein or TRD-70k (i.e., fluorescent probe, texas red (TR)-labeled dextran with average molecular weight of 70k), we used buffer A supplemented with 1.0 mM calcein or with 10 μM TRD-70k for the GUV preparation procedure. After purification, the GUV suspension (~300 μL) was transferred into a handmade microchamber, which had been formed on a glass slide by inserting a U-shaped silicone-rubber spacer between a coverslip and the glass slide.[19] To prevent strong interaction between the glass surface and GUVs, the inside of the microchamber was coated with 0.10%(w/v) BSA in buffer A.[10] The GUVs were observed using an inverted fluorescence phase-contrast microscope (IX-70, Olympus, Tokyo, Japan) maintained at 25 ± 1 °C under the control of a stage thermocontrol system (Thermoplate, Tokai Hit, Shizuoka, Japan).[24]

Various concentrations of Lfcin B solution in buffer A containing 0.10 M glucose were continuously added in the vicinity of a GUV through a ~ 20-μm-diameter glass micropipet positioned using a micromanipulator. The distance between the GUV and the tip of the micropipet was ~70 μm, and the

DOI: 10.1021/acs.biochem.5b00594
Biochemistry 2015, 54, 5802−5814

applied pressure, ΔP (= $P_{in} - P_{out}$, where P_{in} and P_{out} were the pressure of the inside and the outside of a micropipet, respectively) was 30 Pa.[19,27] Phase-contrast and fluorescence images of GUVs were recorded using a high-sensitivity EM-CCD camera (C9100−12, Hamamatsu Photonics K.K., Hamamatsu, Japan) with a hard disk. Three ND filters were used to decrease the intensity of the incident light, resulting in conditions where almost no photobleaching of fluorescent probes in a GUV occurred during the interaction of the Lfcin B solution with single GUVs. Thus, under these conditions, the decrease in fluorescence intensity inside a GUV corresponded to leakage of the fluorescent probes from the inside to the outside of the GUV. The fluorescence intensity inside the GUVs was determined using the AquaCosmos software (Hamamatsu Photonics K.K.), and the average intensity per GUV was estimated. The details of this method is described in our previous reports.[19,27]

To obtain the rate constant of the Lfcin B-induced pore formation in lipid membranes (k_p) for various GUVs, the time course of fraction of intact GUV was fit by the exponential decay function using Origin Pro (ver. 8.5, Origin Lab. Corp., Northampton, MA, USA). Three independent experiments were carried out at each Lfcin B concentration to obtain the rate constant, and for each experiment ∼20 single GUVs were analyzed to evaluate the rate constant. Mean values and standard errors of the rate constant among the three experiments were calculated.

Measurement of Particle Size during the Interaction of Lfcin B with PG/PC (1/1)-LUV. The size of the LUVs in buffer A was measured at 25 °C using a dynamic light scattering (DLS) apparatus (Zetasizer Nano ZS, Malvern Instrument Ltd., Worcester, UK).[36] PG/PC (1/1)-LUVs were prepared by the extrusion method using a 100 nm-pore-size nuclepore membrane.[24] Each of the solutions (buffer A, peptide solution, and the LUV suspension) were filtered through a 0.2 μm-pore-size filter (DISMIC-25AS, Advantec Toyo Kaisha Ltd., Tokyo, Japan). The mean particle diameter (Z-average) of the LUVs was obtained by the cumulant method.

RESULTS AND DISCUSSION

MIC of Lfcin B against *E. coli*. First we investigated the antimicrobial activity of the Lfcin B prepared in our laboratory. Using the standard method, we determined the MIC of Lfcin B against *E. coli* (JM-109) as 3 ± 1 μM. This value is consistent with the previously reported value for *E. coli* (0111) (2 μM).[3]

Lfcin B-Induced Influx of SYTOX Green into Cytoplasm of *E. coli*. To clarify the target of Lfcin B's bactericidal activity against *E. coli*, we investigated permeabilization of the plasma membrane of *E. coli* by measuring the influx of the membrane-impermeant fluorescent probe, SYTOX green, into the bacterial cytoplasm.[37,38] Notably, the fluorescence of SYTOX green is elevated upon binding to nucleic acids; thus increased fluorescence intensity indicates influx of the marker into the cytoplasm. As shown in Figure 1A, the fluorescence intensity of SYTOX green increased rapidly with time during the incubation of SYTOX green with an *E. coli* suspension; the increment of the fluorescence intensity also increased with increasing Lfcin B concentration (from 0 to 50 μM). For a given Lfcin B concentration, the increment of the fluorescence intensity rose with decreasing bacterial density; e.g., the SYTOX influx at 600 s increased 4 fold when the bacterial density decreased from 1.0×10^6 to 1.0×10^5 CFU/mL (Figure 1B).

Thus, the results of Figure 1 indicate that during the interaction of *E. coli* with Lfcin B its plasma membrane was rapidly damaged, and as a result SYTOX green permeabilized through the plasma membrane to enter the inside of *E. coli*. This suggests that bactericidality reflects the Lfcin B-induced damage of *E. coli* plasma membrane. Figure 1A shows that the fraction of bacteria with damaged plasma membrane increased with an increase in Lfcin B concentration in the buffer outside the bacteria. Figure 1B shows that the fraction of bacteria with damaged plasma membrane increased with a decrease in the bacterial density. This can be explained by the decrease in the effective concentration of Lfcin B in the buffer outside the bacteria with an increase in bacterial density because binding of Lfcin B to the membranes of bacteria decreases the Lfcin B concentration in the buffer. A similar phenomena was observed when peptides interact with LUVs in a suspension (see the below section).[19]

Induction of Calcein Leakage from PG/PC (1/1)-LUVs by Lfcin B. To examine directly membrane damage by Lfcin B and to confirm the target of Lfcin B, we investigated the interaction of Lfcin B with PG/PC (1/1)-LUVs encapsulating a water-soluble fluorescent probe (calcein) using the standard LUV suspension method. Figure 2A shows the time course of

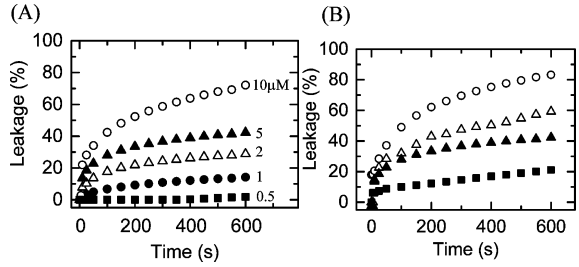

Figure 2. Lfcin B-induced leakage of calcein from LUVs. (A) Time course of Lfcin B-induced leakage of calcein from a suspension of PG/PC (1/1)-LUVs after addition of various concentrations of Lfcin B at 25 °C. Final Lfcin B concentration is described at the right of each curve. Lipid concentration was 25 μM. (B) Time course of 5.0 μM Lfcin B-induced leakage of calcein from suspensions of various concentrations of PG/PC (1/1)-LUVs at 25 °C. Lipid concentrations were 1.6 μM (○), 2.5 μM (△), 25 μM (▲), and 380 μM (■).

the leakage (i.e., the efflux) of calcein from the inside of the LUVs following exposure to various concentrations of Lfcin B. The fraction of leakage increased with time over 10 min for 1.0 to 10 μM Lfcin B, and the rate of leakage increased with Lfcin B concentration. At concentrations of ≤0.50 μM Lfcin B, no leakage was observed over 10 min. In contrast, the rate of leakage induced at a higher concentration of Lfcin B (5.0 μM) increased with a decrease in lipid concentration (i.e., LUV concentration) (Figure 2B).

These results indicated that Lfcin B induced damage of membrane structure of the LUVs, thereby causing leakage of calcein from the inside of the LUVs. However, there can be many causes for the leakage of water-soluble fluorescent probes, such as pore formation, membrane fusion, large shape changes, and vesicle rupture; it can be difficult to identify the cause of the leakage based on the results of the LUV suspension method.[19] We also noted that the rate of leakage correlated negatively with increase of lipid concentration. This can be explained by the decrease in the effective concentration of Lfcin B in the buffer with an increase in LUV concentration because

DOI: 10.1021/acs.biochem.5b00594
Biochemistry 2015, 54, 5802−5814

binding of Lfcin B to the LUV membranes decreases the Lfcin B concentration in the buffer.[19]

Induction of Calcein Leakage from PG/PC (1/1)-GUVs by Lfcin B. To elucidate the process of Lfcin B-induced leakage of calcein from the LUVs, we investigated the interaction of Lfcin B with single PG/PC (1/1)-GUVs containing calcein and 0.10 M sucrose using the single GUV method.[19,23] The interaction was carried out in buffer A containing 0.10 M glucose at 25 °C. During observation of a single GUV by phase-contrast fluorescence microscope, the tip of a micropipet was approached to the GUV at t = 0, and the Lfcin B solution was continuously added from the micropipet into the vicinity of the GUV. Figure 3A shows typical

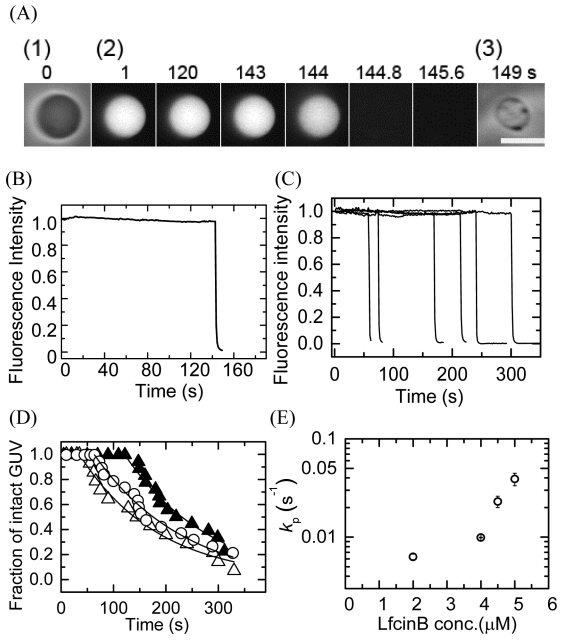

Figure 3. Membrane permeation of calcein from single PG/PC (1/1)-GUVs induced by Lfcin B. (A) Leakage of calcein from single PG/PC (1/1)-GUVs was induced by 2.0 μM Lfcin B in buffer A at 25 °C. Fluorescence images (2) show that the calcein concentration inside the GUV rapidly decreased after the addition of Lfcin B. The numbers above each image show the time in seconds after the Lfcin B addition was started. Also shown are phase contrast images of the GUV at time 0 (1) and 149 s (3). The bar corresponds to 20 μm. (B) Time course of the change in the normalized fluorescence intensity of the GUV shown in (A). We defined the normalized fluorescence intensity of the intact GUV before the initiation of the membrane permeation as 1.0. (C) Other examples of the time course of the change in the normalized fluorescence intensity of several "single GUVs" under the same conditions as in (A). (D) Time course of fraction of intact GUV, P_{intact}, of PG/PC (1/1)-GUV. (Δ) shows the data including the results shown in (C). (○) and (▲) show the time course of P_{intact}, of other independent experiments. Solid lines represent the best fit curves of eq 1. (E) Lfcin B concentration dependence of the rate constant of pore formation, k_p. Mean values and standard errors are shown.

experimental results following the interaction of a single GUV with 2.0 μM Lfcin B. Prior to Lfcin B addition, a phase-contrast microscopic image of the GUV indicated a high contrast in the GUV (Figure 3A-1) due to the difference in the saccharide concentrations between the inside (0.10 M sucrose) and the outside (0.10 M glucose) of the GUV. A fluorescence microscopic image of the same GUV (Figure 3A-2) showed a high concentration of calcein inside the GUV at this time. During the addition of the 2.0 μM solution of Lfcin B, the fluorescence intensity inside the GUV was almost constant over the first 143 s, following which the fluorescence intensity decreased suddenly (Figure 3A-2,B). After 146 s the fluorescence intensity fell to effectively zero; a phase-contrast image of the same GUV (Figure 3A-3) showed that the spherical GUV structure remained, albeit with an apparent decrease in diameter. As discussed in our previous reports,[23−25] the rapid decrease in fluorescence intensity occurred as a result of the leakage of the fluorescent probe through the peptide/protein-induced pores in the lipid membranes. Thus, the time at which the fluorescence intensity began to rapidly decrease corresponded to the time at which a pore was formed in the membrane. When the same experiments were carried out using 20 single GUVs, we observed a stochastic occurrence of a similar rapid leakage of calcein from each GUV (Figure 3C).

The concentration of fluorescent probe inside a GUV is proportional to the fluorescence intensity of the inside of the GUV. In the time course of fluorescence intensity inside the GUV (such as Figure 3B,C), the time when the normalized fluorescence intensity inside the GUV starts to decrease corresponds to the time of pore formation in the lipid membrane. In other words, if the normalized fluorescence intensity inside the GUV is 1.0, no leakage of the fluorescent probe occurs, and therefore the state of this GUV corresponds to the intact state. On the other hand, if the normalized fluorescence intensity is less than 1.0, some leakage of the fluorescent probe occurs, and therefore the state of this GUV corresponds to the pore state. As we demonstrated in our previous papers on peptide-induced pore formation,[23−25] the rate constant of Lfcin B-induced pore formation in lipid membranes can be obtained by analyzing the time course of the fraction of intact state of GUVs (i.e., those from which the fluorescent probe did not leak) among the examined GUVs, $P_{intact}(t)$, over time t. Figure 3D (Δ) shows that the value of P_{intact} of PG/PC (1/1)-GUVs decreased with time during the interaction with 2.0 μM Lfcin B. The curve of the time course of P_{intact} (Δ) was well fit by a single exponential decay function defined by eq 1, as follows,

$$P_{intact}(t) = \exp\{-k_p(t - t_{eq})\} \quad (1)$$

where k_p is the rate constant of the Lfcin B-induced pore formation and t_{eq} is a fitting parameter which denotes the time required for the binding equilibrium of LfcinB from aqueous solution to the GUV membrane.[23,28] To determine the mean value for k_p, three independent experiments (n = 3) using 20 single GUVs to obtain the time course of P_{intact} were carried out, and these curves were also well fit by eq 1 (Figure 3D). The mean value of k_p for 2.0 μM Lfcin B was (6.3 ± 0.5) × 10^{-3} s^{-1} (n = 3). The values of the fitting parameter t_{eq} have larger variation compared with those of k_p. The value of t_{eq} includes the time required for attaining equilibrium concentration of LfcinB in the vicinity of a GUV because we started to add the LfcinB solution from the tip of the micropipet to the vicinity of a GUV at t = 0. Therefore, the value of t_{eq} depends on the size and the shape of the micropipet tip and the setting of micropipet inside a microchamber, which have some variation in each experiment. This is one of the main reasons for the larger variation of t_{eq}.

We also investigated the effect of Lfcin B concentration on the rate constant of pore formation. At concentrations of ≥1.0 μM Lfcin B, leakage of calcein like that shown in Figure 3C was observed. We used this assay to determine the rate constant of

DOI: 10.1021/acs.biochem.5b00594
Biochemistry 2015, 54, 5802−5814

pore formation (k_P) at concentrations of ≥2.0 μM Lfcin B (Figure 3E). k_P increased with Lfcin B concentration. At 4.5 and 5.0 μM k_P values were greater than 2×10^{-2} s^{-1}.

Lfcin B-Induced Structural Change in Single PG/PC (1/1)-GUVs. To elucidate the decrease in diameter of the GUVs after its interaction of LfcinB, we investigated the process of the structural change of single GUVs using the phase contrast microscopy. Figure 4A shows a typical example of 5.0 μM Lfcin

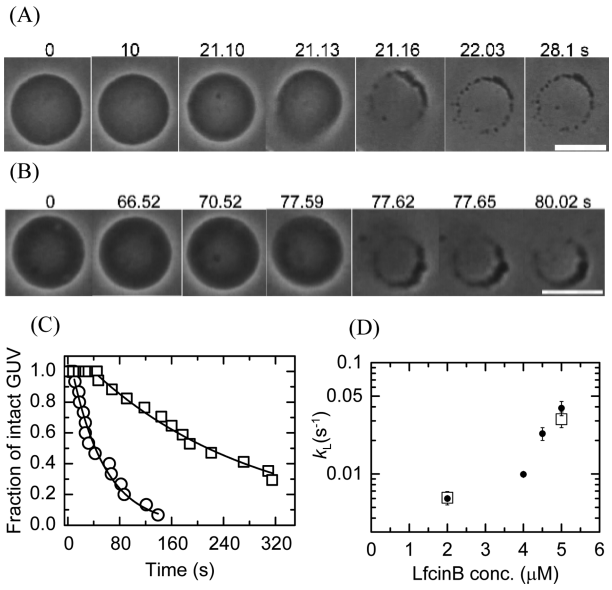

Figure 4. Structural change of single PG/PC (1/1)-GUVs induced by Lfcin B. Phase contrast images of single GUVs in the interaction of (A) 5.0 μM and (B) 2.0 μM Lfcin B in buffer A at 25 °C. The numbers above each image show the time in seconds after the Lfcin B addition was started. The bar corresponds to 20 μm. (C) Rate constant of Lfcin B-induced local rupture of PG/PC (1/1)-GUVs. Time course of the fraction of intact GUVs which was identified by its phase-contrast microscopic image, $P_{intact}(t)$, in the presence of 2.0 μM (□) and 5.0 μM (○) Lfcin B. (D) The Lfcin B concentration dependence of the rate constant of local rupture, k_L (□). For comparison, the Lfcin B concentration dependence of the rate constant of pore formation, k_P, (the same as Figure 3E) was also plotted (●).

B-induced transformation of a PG/PC (1/1)-GUV. As shown in phase-contrast microscopic images in Figure 4A, at 21.13 s the sucrose solution inside the GUV suddenly started to diffuse to the outside of the GUV. From 21.13 to 21.16 s, the diameter of the GUV rapidly decreased; from 21.16 s, the diffusional flow of sucrose solution could not be observed. At 21.16 s the phase contrast of the inside of the GUV became small: although the spherical shape of the GUV was still visible, a large area of thicker membrane region with higher contrast and several small high-contrast (black) particles appeared on the membrane of the GUV. Figure 4B shows a typical example of the 2.0 μM Lfcin B-induced transformation of a PG/PC (1/1)-GUV. Similar structural changes were observed in this GUV, including the rapid leakage of sucrose, but the leakage process started at 77.59 s and completed at 77.65 s within 66 ms.

The results of Figure 4 clearly indicate that LfcinB induced a transient, rapid leakage of sucrose from the single GUVs and then smaller spherical GUVs remained. We infer that part of the GUV membrane was lost and postulate that the large areas of the thicker, increased-contrast membrane and small high-contrast (black) particles on the membrane correspond to a complex of lipid membranes and Lfcin B (see the details in the Discussion section). Because of the very fast leakage, and at the present time resolution of the experiments (33 ms), we could not follow the evolution of pore as we did in other similar studies.[28] Several words have been used to explain such a rapid leakage of sucrose; large pore formation, local rupture, burst of membranes, and rupture of membranes. Because of the limited time-resolution (i.e., 33 ms) in our experimental system, we could not reveal detailed structural changes of the GUV during the rapid leakage of sucrose. Therefore, at present stage we cannot identify the elementary processes and the mechanism of the rapid leakage. Here we use the word of "local rupture" tentatively to express the rapid leakage of sucrose and the survival of spherical structure of GUVs. Previously, this word (local rupture) was used for the similar phenomena induced by a peptide, transportan 10.[39]

Our results suggested that the leakage of calcein from inside single GUVs occurred as a result of local rupture in the GUV membranes. To confirm the correlation between the leakage of calcein and local rupture in GUVs, we calculated the rate constant of local rupture. For this calculation, we considered the conversion from the intact state of GUV to the ruptured state of GUV in which sucrose has been already leaked or is leaking as a two-state transition. The concentration of sucrose inside a GUV is proportional to the phase contrast of the inside of the GUV. In the consecutive phase contrast images (such as Figure 4A,B) at the time resolution of 33 ms, the time of the image in which the rapid leakage of sucrose started from a GUV (e.g., 21.13 s in Figure 4A and 77.59 s in Figure 4B) corresponds to the time of local rupture. Therefore, the state of the GUV before the time of local rupture corresponds to the intact state, and the state of the GUV at and after this time corresponds to the ruptured state. The rate constant of the two-state transition from the intact state to the rupture state (i.e., the rate constant of local rupture), k_L, can be determined from the fraction of intact state of GUVs (i.e., the fraction of intact GUVs), designated as $P_{intact}(t)$. Figure 4C shows the time course of $P_{intact}(t)$ in the presence of 2.0 μM Lfcin B. The fraction of the intact GUV can be expressed using the rate constant, k_L, as follows:

$$P_{intact}(t) = \exp\{-k_L(t - t_{eq})\} \quad (2)$$

where t_{eq} is an adjustable parameter. This equation is almost the same as that for the rate constant of the EGCg-induced burst of a GUV.[28] All the curves of the time course of the $P_{intact}(t)$ were well fit by eq 2 (Figure 4C). The rate constant k_L increased with increasing Lfcin B concentration: at 2.0 and 5.0 μM Lfcin B, the k_L values were $(7.0 \pm 0.2) \times 10^{-3}$ s^{-1} and $(3.6 \pm 0.2) \times 10^{-2}$ s^{-1}, respectively (n = 3 for each concentration). These results indicated that the Lfcin B-induced local rupture in the GUV membrane apparently followed the first-order reaction. The values of k_L and k_P against Lfcin B concentrations were the same within an experimental error (Figure 4D). These results clearly indicate that the leakage of calcein from the inside to the outside of single GUVs occurred as a result of local rupture in the GUV membrane and that the smaller sizes of pores were not formed before the local rupture. This result supports the above hypothesis on the two-state transition for the formation of the local rupture.

Induction of TRD-70k Leakage from PG/PC (1/1)-GUVs by Lfcin B. In order to examine the size of the Lfcin B-induced pores in lipid membranes, we investigated the leakage of a water-soluble fluorescent probe, TRD-70k, using the single

DOI: 10.1021/acs.biochem.5b00594
Biochemistry 2015, 54, 5802−5814

GUV method. The molecular weight distribution of TRD-70k is 60000−90000 according to the manufacturer, and its Stokes−Einstein radius, R_{SE}, is 6.4 nm.[40] Figure 5A shows the

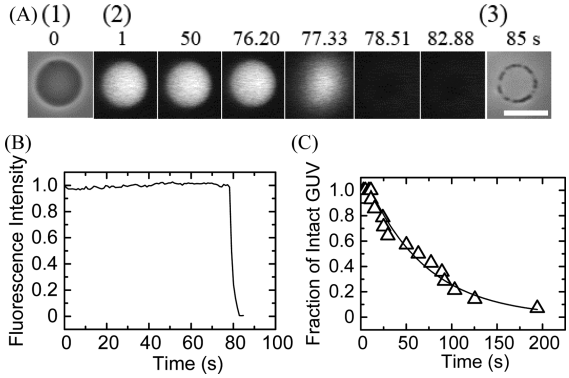

Figure 5. Membrane permeation of TRD-70k from single PG/PC (1/1)-GUVs induced by Lfcin B. (A) Leakage of TRD-70k from single PG/PC (1/1)-GUVs induced by 5.0 μM Lfcin B in buffer A at 25 °C. (A) Fluorescence images (2) show that the TRD-70k concentration inside the GUV rapidly decreased during the addition of Lfcin B. The numbers above each image show the time in seconds after Lfcin B addition was started. Also shown are phase contrast images of the GUV at time 0 (1) and 85 s (3). The bar corresponds to 20 μm. (B) Time course of the change in the normalized fluorescence intensity of the GUV shown in (A). (C) Time course of P_{intact} of PG/PC (1/1)-GUV containing TRD-70k in the presence of 5.0 μM Lfcin B in buffer A at 25 °C. The solid line represents the best fit curve using eq 1.

effect of 5.0 μM Lfcin B on single PG/PC (1/1)-GUVs preloaded with TRD-70k. Prior to Lfcin B addition, a phase-contrast microscope image of the GUV showed high contrast (Figure 5A-1) due to the difference in the saccharide concentration between the inside (0.1 M sucrose) and the outside (0.1 M glucose) of the GUV. A fluorescence microscope image of the same GUV (Figure 5A-2) showed a high concentration of TRD-70k inside the GUV at this time. During addition of a 5.0 μM solution of Lfcin B, the fluorescence intensity inside the GUV remained similar over the first 77.30 s, but at 77.33 s a rapid decrease in the fluorescence intensity was observed (Figure 5A-2,B). After 82.89 s, the fluorescence intensity approached zero, although a phase-contrast image of the same GUV (Figure 5A-3) showed that the GUV retained its spherical structure, albeit with a decreased diameter. These data indicate that TRD-70k passed through Lfcin B-induced pores in the GUV membrane. When the same experiments were carried out using 20 single GUVs, similar leakage of TRD-70k from a GUV was observed to occur in a stochastic fashion. Figure 5C shows that the curve of the time course of P_{intact} was well fit by eq 1. The average value of k_p for 5.0 μM Lfcin B was $(2.1 \pm 0.4) \times 10^{-2}$ s^{-1} (n = 3). This k_p value is smaller than that obtained using PG/PC (1/1)-GUVs containing calcein. On the basis of the results of Figures 4 and 5, we infer that the radius of the Lfcin B-induced pore is greater than 6.4 nm (i.e., R_{SE} of TRD-70k).

Effects of Electrostatic Interactions on Lfcin B-Induced Pore Formation in Single PG/PC-GUVs. It has been reported that the binding constant of Lfcin B with lipid membranes increases with an increase in contents of negatively charged lipids such as phosphatidylglycerol,[20,21] suggesting that the electrostatic interactions between Lfcin B and the lipid membrane play an important role in the binding of Lfcin B. To control electrostatic interactions of lipid membranes in water, we can change surface charged density of the membranes or salt concentrations.[41−43] The surface charge density can be controlled by the concentration of negatively charged lipid (i.e., PG) in the PG/PC membranes. First, to elucidate the effects of the surface charge density on the Lfcin B-induced pore formation, we investigated the interaction of Lfcin B with single PG/PC (1/4)-GUVs containing calcein. Lfcin B at concentrations of ≤5.0 μM did not induce calcein leakage. However, at concentrations of ≥10 μM Lfcin B, leakage of calcein similar to that seen in Figure 3A,C was observed. Figure 6A shows the time course of P_{intact} of PG/PC (1/4)-GUVs

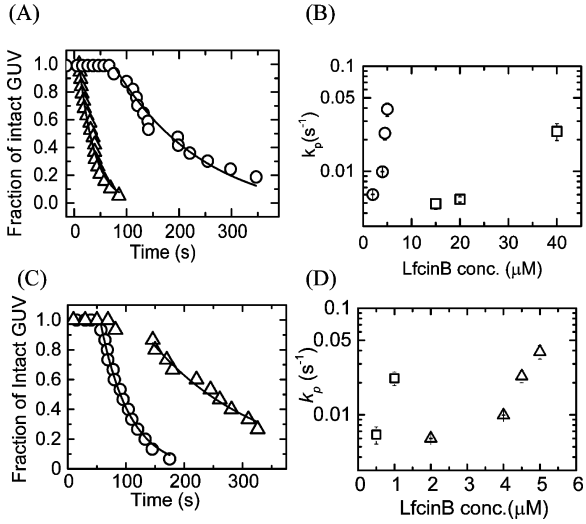

Figure 6. Effects of electrostatic interactions on Lfcin B-induced pore formation. (A) Time course of P_{intact} of PG/PC (1/4)-GUV containing calcein in buffer A during the interaction of various concentrations of Lfcin B. (Δ) 40 μM, and (○) 20 μM Lfcin B. Solid lines represent the best fit curves of eq 1. (B) The Lfcin B concentration dependence of the rate constant of pore formation, k_p in PG/PC (1/4)-GUV (□). For comparison, the same data for PG/PC (1/1)-GUV was also plotted (○) (this is the same data as in Figure 3E). Mean values and standard errors were shown. (C) Time course of P_{intact} of PG/PC (1/1)-GUV containing calcein in buffer A without NaCl (10 mM PIPES, pH 7.0, 1.0 mM EGTA) during the interaction of various concentrations of Lfcin B. (○) 1.0 μM, and (Δ) 0.5 μM Lfcin B. A solid line represents the best fit curve of eq 1. (D) The Lfcin B concentration dependence of the rate constant of pore formation, k_p in PG/PC (1/1)-GUV in buffer A without NaCl (10 mM PIPES, pH 7.0, 1.0 mM EGTA) (□). For comparison, the same data for PG/PC (1/1)-GUV was also plotted (Δ) (this is the same data as in Figure 3E). Mean values and standard errors were shown.

interacting with various concentrations of Lfcin B; these data were well fit by eq 1. For example, the mean value of k_p for 20 μM Lfcin B was $(5.4 \pm 0.3) \times 10^{-3}$ s^{-1} (n = 3). As shown in Figure 6B, at concentrations of ≥15 μM Lfcin B, the rate constant of pore formation k_p was determined and k_p increased with Lfcin B concentration. It is evident that higher concentrations of Lfcin B were required to induce pore formation in PG/PC (1/4)-GUVs than in PG/PC (1/1)-GUVs. This result suggests that the activity of Lfcin B-induced pore formation increases with the surface charge density of the membrane. As an alternative explanation, the PG concentration, rather than the surface charge density, may play a role in Lfcin B-induced pore formation.

DOI: 10.1021/acs.biochem.5b00594
Biochemistry 2015, 54, 5802−5814

Next, to elucidate the effects of the salt concentration on the Lfcin B-induced pore formation, we investigated the interaction of Lfcin B with single PG/PC (1/1)-GUVs in buffer A without NaCl (10 mM PIPES, pH 7.0, 1.0 mM EGTA). At concentrations of ≥1.0 μM Lfcin B, leakage of calcein similar to that seen in Figure 3A,C was observed. Figure 6C shows the time course of P_{intact} of PG/PC (1/1)-GUVs interacting with various concentrations of Lfcin B; these data were well fit by eq 1. As shown in Figure 6D, the mean value of k_P for 1.0 μM and 0.5 μM Lfcin B were $(2.2 \pm 0.3) \times 10^{-2}$ s^{-1} (n = 3) and $(6.5 \pm 1.2) \times 10^{-3}$ s^{-1} (n = 3), respectively. It is evident that lower concentrations of LfcinB induced pore formation in buffer A without NaCl than that in buffer A containing 150 mM NaCl (i.e., the k_p values in 0 mM NaCl were greater than those in 150 mM NaCl). Electrostatic interactions in buffer increase with a decrease in salt concentration because shielding of the membrane surface charge by counterions decreases (i.e., the Debye length increases),[41,43] so Figure 6D indicates that k_p increases with an increase in the extent of electrostatic interactions.

Both the results of the effect of the surface charge density and that of salt concentration on k_p clearly show that k_p increases with an increase in the extent of electrostatic interactions due to membrane surface charges. One of main factors of the binding of Lfcin B with PG/PC membranes is the electrostatic attraction between the positively charged peptide and the negatively charged membranes. This electrostatic interaction increases with an increase in surface charge density (i.e., the increase of the negatively charged DOPG concentration) or a decrease in salt concentration. Therefore, when Lfcin B concentration in buffer is the same, its surface concentration in the membrane increases with an increase in the electrostatic interaction. It is reported that the surface concentration of magainin 2 determines the rate constant of pore formation for the interaction of positively charged magainin 2 with negatively charged PG/PC membranes.[25] Therefore, the results in Figure 6 suggest that the surface concentration of Lfcin B is one of key factors for pore formation.

Lfcin B-Induced Shape Changes in Single PG/PC (1/4)-GUVs. To elucidate how Lfcin B interacts with the PG/PC membranes, we investigated its effect on the shapes of PG/PC (1/4)-GUVs upon addition of Lfcin B. It is well-known that analysis of substance-induced shape changes of GUVs is a highly sensitive method for detecting the interaction of substances with lipid membranes.[44−48] Generally, there are various shapes of GUVs such as sphere, prolate, cylinder, and discocyte. The shapes of GUVs are determined based on some parameters such as area difference between outer and inner monolayers and the volume to the area ratio of the GUV when they are formed. We can select GUVs based on their shape depending on the purpose of experiments. In this report we selected spherical GUVs for leakage experiments and prolate GUVs for shape change experiments. The probability of formation of prolates in PG/PC (1/1)-GUVs was much lower than that of PG/PC (1/4)-GUVs. Hence here we investigated the effects of the interaction of Lfcin B with membranes on the shape of prolate PG/PC (1/4)-GUVs. In the absence of Lfcin B, a GUV had a prolate shape (Figure 7(1)). After starting the addition of 0.20 μM Lfcin B, the GUV changed into a pear-like structure (Figure 7 (2)), subsequently changed into the shape of two-spheres-connected by a neck (Figure 7 (3)). We observed this shape change in 7 of 8 examined GUVs. In order to determine the reversibility of this shape change, the addition of Lfcin B was stopped after the complete shape change of the GUV, and observation was continued. Figure 7 (4)−(6) show the time course of the shape change of the GUV after the addition of Lfcin B was stopped. First, the two-spheres-connected by a neck changed into a pear (Figure 7 (5)); the pear then reverted into a prolate shape (Figure 7 (6)). We can reasonably consider that after the addition of Lfcin B was stopped, remaining Lfcin B diffused away from the vicinity of the GUV into the bulk solution, inducing a decrease in the Lfcin B concentration near the GUV; the local concentration of peptide in the membrane presumably then decreased (i.e., Lfcin B molecules in the outer monolayer of the GUV transferred into the aqueous solution). This result indicates that the shape change in PG/PC (1/4)-GUV induced by addition of 0.20 μM Lfcin B was reversible. The threshold concentration of Lfcin B for the shape change from a prolate to two spheres connected by a neck (i.e., the Lfcin B concentration at which the shape change occurred in 50% of examined GUVs) was 0.15 μM. We observed the reversibility of the shape change in all the examined GUVs (n = 7).

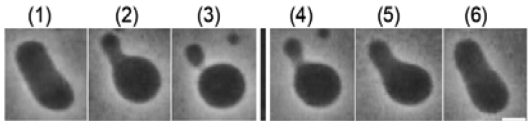

Figure 7. Shape change of a PG/PC (1/4)-GUV induced by the interaction of Lfcin B and its reversibility. (1)−(3) After the addition of 0.20 μM Lfcin B, a prolate changed into a pear, and then into a two spheres connected by a narrow neck. The time after the addition of Lfcin B through the micropipet is (1) 0 s, (2) 66 s, and (3) 82 s. (4)−(6) After the addition of Lfcin B was stopped, the shape change was reversed. The time after stopping the addition of Lfcin B is (4) 125 s, (5) 151 s, and (6) 208 s. The bar corresponds to 10 μm.

The results in Figure 7 clearly show that low concentrations of Lfcin B (well below the threshold concentration of pore formation of GUV) induced shape changes in PG/PC (1/4)-GUVs. What is the mechanism for these shape changes? It is well established that the shape of a GUV is determined by the minimization of the elastic energy of the closed membrane and that the "area-difference-elasticity" model (ADE model) reasonably explains shape changes of GUVs.[49,50] In the ADE model, the area of each monolayer is not fixed to the equilibrium area, but the monolayer membrane can stretch elastically to increase the membrane's nonlocal elastic energy. Thus, the elastic energy of the GUV (W_{el}) can be expressed as a sum of the membrane bending energy and the energy of the relative monolayer stretching. In the ADE model, the shape of the GUV is determined by the minimization of the membrane elastic energy (W_{el}) for a given area A, volume V, and the difference ($\Delta A_0 (= A_0^{out} - A_0^{in})$) between the area of the outer (A_0^{out}) and the inner monolayers (A_0^{in}) in the GUV bilayer membrane under the relaxed (i.e., nonstretched) condition.[49,50] An analysis based on the ADE model shows that, under the condition of constant volume of the GUV, the shape changes as follows: as ΔA_0 increases, prolate → pear → two-spheres-connected by a narrow neck. These shape changes are the same as those induced by Lfcin B in the PG/PC (1/4)-GUVs (Figure 7). This analysis therefore indicates that the interaction of Lfcin B with a GUV increased ΔA_0 of the GUVs. We hypothesize that A_0^{in} of the GUV does not change. Therefore, we can reasonably consider that the binding of Lfcin B induces an increase in the area of the outer monolayer, A_0^{out}. Moreover, the

DOI: 10.1021/acs.biochem.5b00594
Biochemistry 2015, 54, 5802−5814

observed reversibility of the Lfcin B-induced shape change indicates that the binding of Lfcin B to the membrane interface is reversible.

Association of PG/PC (1/1)-LUVs by Lfcin B. To examine the interaction of PG/PC (1/1) membranes with Lfcin B, we used DLS to determine a time course of the LUV sizes. We used PG/PC (1/1)-LUVs with diameters of 115 nm (Z-average) in buffer A. After mixing with various concentrations of Lfcin B solution (final concentration from 0.50 to 1.0 μM), the average LUV diameter increased with time (Figure 8). At

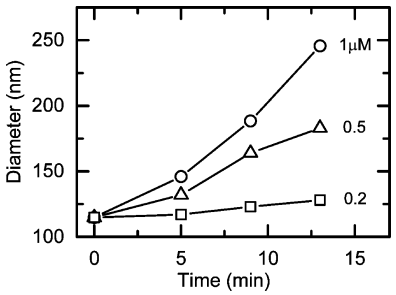

Figure 8. Time course of the average particle diameter (Z-average) in the LUV suspension. Various concentrations of Lfcin B solution were mixed with PG/PC (1/1)-LUV suspension at t = 0. Final Lfcin B concentration is described at the right of each curve. Final lipid concentration was 38 μM. The size distributions were obtained using the non-negative least-squares method.

13 min after the mixing, the Z-average values of the LUV suspensions containing 1.0 μM and 0.50 μM LfcinB were 246 and 183 nm, respectively. At concentrations of ≤0.20 μM Lfcin B, no significant increase in LUV diameter was observed. After 100 fold dilution of these LUV suspensions with the buffer, Z average values of the suspensions for 1.0 μM and 0.50 μM LfcinB decreased to 118 nm, which is almost the same as the initial diameter of the LUVs (115 nm). This result indicates that LfcinB-induced increase in the size of LUVs are almost reversible.

We can compare this result with that of Figure 2A because lipid concentrations in both experiments were similar (i.e., 25 and 38 μM in the experiments shown in Figures 2A and 8, respectively). Notably, 0.50 μM Lfcin B (i.e., peptide/lipid ratio, P/L, equals 0.020) did not induce leakage of calcein (Figure 2A), nonetheless 0.50 μM Lfcin B (i.e., P/L = 0.013) increased the average LUV diameter (Figure 8). Generally the increase in the size of LUVs occurs due to associations of LUVs and membrane fusions of LUVs. It is considered that the first stage of most membrane fusions is association of LUVs, and the second step is the fusion between the associated LUVs. In most cases the association is reversible; i.e., if we decrease the concentration of substances inducing the association, the LUVs are separated each other.[51] For the second step (i.e., membrane fusion), another factor or longer time is required. The above results of the dilution of the samples indicated that the increase in LUV diameter is due to mostly reversible association of LUVs and partly fusion of LUVs. This is consistent with the result of the reversible binding of LfcinB to the GUV membrane indicated by the experiments of the shape change of the GUVs. Therefore, the results in Figure 8 indicates that after the interaction of Lfcin B with LUV membranes, the LUVs associated each other, and thus the average size of the LUVs increased with time. The rate of the association increased with an increase in Lfcin B concentration.

General Discussions. The results of SYTOX green experiments suggest that the Lfcin B-induced damage of *E. coli* plasma membrane to cause membrane permeabilization of SYTOX green is a main cause of death of *E. coli*. The mechanism of the bactericidal activity of Lfcin B is still controversial. Some researchers have suggested that Lfcin B enters the bacterial cytoplasm via translocating plasma membrane, in a manner like that of cell-penetrating peptides, and then acts on DNA, which is a main cause of Lfcin B's bactericidal activity (see the detailed discussion later).[3] However, our results of SYTOX green experiments directly indicate that the Lfcin B-induced damage of the plasma membrane is more plausible for the mechanism of bactericidal activity than the above hypothesis. To elucidate the mechanism of the Lfcin B-induced damage of plasma membrane, it is indispensable to examine directly membrane damage by Lfcin B and to confirm the target of Lfcin B. For this purpose, we investigated the interaction of Lfcin B with the LUVs of pure lipid membranes. The results showed that Lfcin B induced leakage of calcein from the inside of the LUVs, indicating damage of membrane structure of the LUVs. However, there are many causes for the leakage, and it is difficult to identify its cause based on the results of the LUV suspension method.[19] To clarify the cause of Lfcin B-induced leakage of calcein from the LUVs, we used the single GUV method[19,23] to investigate the interaction of Lfcin B with calcein-containing PG/PC-GUVs. We observed that a rapid leakage of calcein from a GUV started stochastically; its statistical analysis provided a rate constant for Lfcin B-induced pore formation, k_P. After the leakage, the spherical GUV structure remained, but its diameter decreased a little. To elucidate this structural change in the GUVs, we investigated the process of the structural change of single GUVs using phase-contrast microscopy. We observed a rapid efflux of sucrose solution from the inside the GUV, which completed less than 66 ms. This result revealed that Lfcin B induced local rupture in the single GUVs, and from the statistical analysis we obtained the rate constant of local rupture, k_L. The values of k_L and k_P against Lfcin B concentrations were the same within an experimental error. On the basis of these results, we concluded that the leakage of calcein from single GUVs occurred as a result of local rupture in the GUVs and that smaller pores inducing leakage of calcein were not formed before local rupture.

In this report, we used the term "local rupture" to express the rapid leakage of sucrose. So far several terms have been used to explain such a rapid leakage of internal contents such as sucrose and calcein: large pore formation, local rupture, burst of membranes, and rupture of vesicles.[28,39,52−54] However, in many cases of substance-induced rapid leakage of internal contents, its elementary processes have not been well revealed due to the limited time-resolution of the experimental systems, and its mechanisms are not well understood. One exception is the external tension-induced rupture of a GUV (after the rupture, the spherical structure of the GUV completely disappeared).[43,53−60] In this case, a part of elementary processes have been successfully revealed,[53−56] and the classical theory[58−60] can explain reasonably that the rupture occurs due to the tension-induced pore formation as follows. Thermal fluctuation in the lateral density of a lipid membrane induces a pre-pore. If the radius of a pre-pore is less than the critical radius, r_a (= Γ/σ), it closes quickly. However, if the radius expands and reaches r_a, the pre-pore transforms into a pore, and then the radius of the pore becomes infinity rapidly, and hence

DOI: 10.1021/acs.biochem.5b00594
Biochemistry 2015, 54, 5802−5814

the rupture of the GUV occurs. It is noted that the tension-induced rupture of a GUV occurs due to a rapid, large pore formation in lipid membranes. In the case of LfcinB-induced pore formation, we could not observe any processes because the local rupture occurred within 33 ms. Further experiments are indispensable to reveal its elementary processes and its mechanism of the Lfcin B-induced local rupture. After that we can rename this phenomena more adequately.

As shown in Figure 4, during local rupture in a GUV, large structural changes occurred rapidly in the GUV; the diameter of the GUV decreased, and a large area of thicker membrane with higher contrast and several small high-contrast (black) particles appeared on the GUV membrane. On the other hand, Lfcin B can induce association of PG/PC membranes due to the electrostatic attraction between the positively charged Lfcin B and the negatively charged PG/PC membranes, which was supported by the results shown in Figure 8. During the local rupture, association of membranes of the GUV may form multilayers locally, which may induce formation of a large area of the thicker membrane region with higher contrast and a small high-contrast (black) particle at several places on the GUV membrane. This model can explain the decrease in the area of the GUV membrane that is indicated by the decrease in GUV diameter. On the other hand, when we investigated the interaction of EGCg, one of antibacterial substances, with single GUVs, we observed similar rapid leakage of calcein and sucrose, and after the leakage spherical GUVs did not remain; instead the GUV converted to a small lump.[28] In this case we succeeded in observing the evolution of a large pore in the GUV membrane (i.e., the instantaneous pore formation and the following decrease in the radius of the pore). After the formation of a large pore, the high-contrast (black) particles or the thick membrane regions appeared on the GUV membrane, and then during the evolution of the pore with a concomitant of the conversion of the GUV to a small lump, the amount of the high-contrast particles increased. The results using the small-angle X-ray scattering (SAXS) indicated that EGCg induced strong attraction of two bilayers and close contact of them at high concentrations of EGCg.[28] Therefore, it is clear that the high-contrast (black) particles are formed due to the EGCg-induced attraction of two bilayers after the large pore formation.

To elucidate the mechanism of Lfcin B-induced pore formation, we investigated the effects of the electrostatic interactions on the Lfcin B-induced pore formation. The rate constants of Lfcin B-induced pore formation in PG/PC (1/1)-GUV were much larger than those in PG/PC (1/4)-GUV. The initial process of the binding of Lfcin B to the surface of lipid membranes is controlled by the electrostatic interaction between highly positively charged Lfcin B and negatively charged lipid membranes. We can reasonably expect that the surface concentration of Lfcin B in PG/PC (1/1)-GUV is larger than that in PG/PC (1/4)-GUV. Thus, the results shown in Figure 6 indicate that the surface concentration of Lfcin B is one of the key factors for pore formation; with an increase in the surface concentration of Lfcin B, the rate constant of Lfcin B-induced pore formation increases. This tendency has been proven experimentally in the case of magainin 2.[25] On the basis of the structure of Lfcin B in aqueous solution (as determined by NMR), Lfcin B forms an amphipathic antiparallel β-sheet; the face containing amino acids with high interfacial hydrophobicity[61] (such as F1, W6, W8, L13, and F25) is expected to interact strongly with the membrane interface if Lfcin B lies in parallel with the membrane surface.[9] Experimental results using quenching of Trp fluorescence indicate that the Trp residues of Lfcin B locate at the membrane interface,[62] suggesting that Lfcin B indeed lies in parallel with the membrane surface.[63] This strong interaction of Lfcin B with the lipid membrane interface is postulated to induce an increase in the area of the outer monolayer of a GUV, which is supported by the results of Lfcin B-induced shape change (Figure 7). We infer that this interaction plays an important role in pore formation.

It is important to compare the results of Lfcin B-induced membrane permeation with those of other AMPs and other antimicrobial substance-induced membrane permeation. Magainin 2 initially induced a large, transient pore in lipid membranes following which the radius of the pore decreased to a stable smaller size,[26] but the diameter of GUVs did not change significantly after magainin 2-induced pore formation.[25,26] For example, high concentrations of magainin 2 induced a small amount (~10% of the total amount) of leakage of TRD-70k only at the initial stage; at the final steady-state, the radius of the magainin 2-induced pore was smaller than 2.8 nm.[26] In contrast, Lfcin B induced complete leakage of TRD-70k (Figure 5). Therefore, we can conclude that the size of the Lfcin B-induced pore is larger than that induced by magainin 2. On the other hand, gomesin, another AMP, induced bursting of GUVs; the structure of GUVs was not observed after the bursting occurred.[52] The authors of that report used the "carpet model" to explain the gomesin-induced disruption of the membrane.[64] Similarly, EGCg induced bursting of GUVs; after such bursting, only a small lump (and not a spherical structure) was observed.[28] With Lfcin B, spherical GUVs (of reduced diameter) were observed after local rupture, suggesting that the mode of damage of lipid membranes due to Lfcin B is different from that of gomesin and EGCg. However, currently we do not know the mechanism of Lfcin B-mediated local rupture. Thus, it is difficult to further contrast the differences in membrane damage caused by these various agents.

As discussed above, some researchers consider that the interaction of Lfcin B with DNA is a main cause of Lfcin B's bactericidal activity.[3] Indeed, lactoferrin has been reported to enter cells and interact with DNA.[65,66] However, it is important to note that even if the main target of an AMP is the plasma membrane of bacteria, the AMP can pass through the induced membrane pore to enter a cell only when the size of the AMP-induced pore is larger than that of the AMP itself. Recently, entry of AMPs into cells by this mechanism was experimentally proven for magainin 2.[26,27] However, the evidence for the entry of peptides/proteins into cells and their binding to DNA does not necessarily indicate that the binding of peptides/proteins to DNA is the main source of bactericidal activity. Notably, some researchers consider that the damage of plasma membrane due to the interaction of Lfcin B with the lipid membrane region is the primary mechanism of this peptide's bactericidal acitivity.[20−22] The results in the present report provide direct experimental evidence to support the latter mechanism. At present, we do not have detailed experimental data to propose the mechanism of the Lfcin B-induced local rupture, but changes in the physical properties of the membrane (such as tension due to high surface concentration of Lfcin B) may play a key role in local rupture. The results of Figure 6 indicates that LfcinB can induce pore formation even if the surface charge density is lower (i.e., 20 mol % DOPG). As described in the introduction, one of the places where Lfcin B molecules attack bacteria is the mammal stomach. The pH of solution in the

DOI: 10.1021/acs.biochem.5b00594
Biochemistry 2015, 54, 5802−5814

stomach is very low (~pH 1−3),[67] and the p*K* of PG is ~pH 3.[68] Hence more than half of PG molecules are protonated (i.e., the surface charge density of plasma membrane of bacteria becomes less than a half of that at neutral pH) in the stomach. Lfcin B does not have negatively charged amino acid residues, and hence its charge density does not change in the stomach. Therefore, we can reasonably consider that LfcinB has antibacterial activity in the stomach.

CONCLUSION

In this report, we provide evidence for Lfcin B-induced rapid damage of the plasma membrane of *E. coli*. Lfcin B induced leakage of calcein from LUVs and GUVs composed of PG/PC membranes, showing direct evidence that Lfcin B caused a damage of these lipid membranes. Using the single GUV method, we observed that Lfcin B induced the rapid leakage of calcein and TRD-70k from single GUVs. After the rapid leakage, the spherical shape of the GUV remained, although its diameter decreased a little, and the GUV membrane contained a large area of thicker membrane region with higher contrast and several small high-contrast particles. At the time resolution of 33 ms, the detailed structural changes of the GUV during the rapid leakage were not revealed. The surface concentration of Lfcin B and the associated physical changes in the membrane, such as stretching of membranes, are among the key factors contributing to pore formation. These results indicate that Lfcin B-induced rapid damage of the plasma membrane of *E. coli* with its concomitant rapid leakage of internal contents is a key factor for the peptide's bactericidal activity.

AUTHOR INFORMATION

Corresponding Author

*Address: Nanomaterials Research Division, Research Institute of Electronics, Shizuoka University, 836 Oya, Suruga-ku, Shizuoka 422-8529, Japan. Tel/Fax: 81-54-238-4741. E-mail: yamazaki.masahito@shizuoka.ac.jp.

Funding

This work was supported in part by a Grant-in-Aid for Scientific Research (B) (No. 15H04361) from JSPS to M.Y. Part of this research was carried out under the Cooperative Research Project of Research Institute of Electronics, Shizuoka University.

Notes

The authors declare no competing financial interest.

ACKNOWLEDGMENTS

This work was carried out in part using instruments at the Molecular Structure Analysis Section of Shizuoka University RIGST.

REFERENCES

(1) Tomita, M., Wakabayashi, H., Shin, K., Yamauchi, K., Yaeshima, T., and Iwatsuki, K. (2009) Twenty-five years of research on bovine lactoferrin applications. *Biochimie 91*, 52−57.

(2) Masson, P. L., Heremans, J. F., and Dive, C. H. (1966) An iron-binding protein common to many external secretions. *Clin. Chim. Acta 14*, 735−739.

(3) Bellamy, W., Takase, M., Yamauchi, K., Wakabayashi, H., Kawase, K., and Tomita, M. (1992) Identification of the bacterial domain of lactoferrin. *Biochim. Biophys. Acta, Protein Struct. Mol. Enzymol. 1121*, 130−136.

(4) Kuwata, H., Yip, T. T., Tomita, M., and Hutchens, T. W. (1998) Direct evidence of the generation in human stomach of an antimicrobial peptide domain (lactoferricin) from ingested lactoferrin. *Biochim. Biophys. Acta, Protein Struct. Mol. Enzymol. 1429*, 129−141.

(5) Yamauchi, K., Tomita, M., Giehl, T. J., and Ellison, R. T., III (1993) Antibacterial activity of lactoferrin and a pepsin-derived lactoferrin peptide fragment. *Inf. Immu. 61*, 719−728.

(6) Tomita, M., Takase, M., Bellamy, W., and Shimamura, S. (1994) A review: The active peptide of lactoferrin. *Acta Paediatr. J. 36*, 585−591.

(7) Gifford, J. L., Hunter, H. N., and Vogel, H. J. (2005) Lactoferricin: a lactoferrin-derived peptide with antimicrobial, antiviral, antitumor, and immunological properties. *Cell. Mol. Life Sci. 62*, 2588−2598.

(8) Eliassen, L. T., Berge, G., Leknessund, A., Wikman, M., Lindin, I., Lokke, C., Ponthan, F., Johnsen, J. I., Sveinbjornsson, B., Kogner, P., Flægstad, T., and Rekdal, Ø. (2006) The antimicrobial peptide, Lfcin B, is cytotoxic to neuroblastoma cells in vitro and inhibits xenograft growth in vivo. *Int. J. Cancer 119*, 493−500.

(9) Hwang, P. M., Zhou, N., Shan, X., Arrowsmith, C. H., and Vogel, H. J. (1998) Three-dimensional solution structure of lactoferricin B, an antimicrobial peptide derived from bovine lactoferrin. *Biochemistry 37*, 4288−4298.

(10) Zasloff, M. (2002) Antimicrobial peptides of multicellular organisms. *Nature 415*, 389−395.

(11) Melo, M. N., Ferre, R., and Castanho, A. R. B. (2009) Antimicrobial peptides: linking partition, activity and high membrane-bound concentrations. *Nat. Rev. Microbiol. 7*, 245−250.

(12) Hwang, P. M., and Vogel, H. J. (1998) Structure-function relationships of antimicrobial peptides. *Biochem. Cell Biol. 76*, 235−246.

(13) Kang, J. H., Lee, M. K., Kim, K. L., and Hahm, K. − S. (1996) Structure-biological activity relationships of 11-residue highly basic peptide segment of bovine lactoferrin. *Int. J. Pept. Protein Res. 48*, 357−363.

(14) Strøm, M. B., Haug, B. E., Rekdal, Ø., Skar, M. L., Stensen, W., and Svendsen, J. S. (2002) Important structural features of 15-residue lactoferricin derivatives and methods for improvement of antimicrobial activity. *Biochem. Cell Biol. 80*, 65−74.

(15) Nguyen, L. T., Schibli, D., and Vogel, H. J. (2005) Structural studies and model membrane interactions of two peptides derived from lactoferricin. *J. Pept. Sci. 11*, 379−389.

(16) Wakabayashi, H., Matsumoto, H., Hashimoto, K., Teraguchi, S., Takase, M., and Hayasawa, H. (1999) N-acylated and D enantiomer derivatives of a nonamer core peptide of lactoferricin B showing improved antimicrobial activity. *Antimicrob. Agents Chemothera 43*, 1267−1269.

(17) Wakabayashi, H., Takase, M., and Tomita, M. (2003) Lactoferricin derived from milk protein lactoferrin. *Curr. Pharm. Des. 9*, 1277−1287.

(18) Hunter, H. N., Demcoe, A. R., Jenssen, T. J., Gutteberg, T. J., and Vogel, H. J. (2005) Human lactoferricin is partially folded in aqueous solution and is better stabilized in a membrane mimic solvent. *Antimicrob. Agents Chemother. 49*, 3387−3395.

(19) Yamazaki, M. (2008) The single GUV method to reveal elementary processes of leakage of internal contents from liposomes induced by antimicrobial substances. *Adv. Planar Lipid Bilayers Liposomes 7*, 121−142.

(20) Aguilera, O., Ostolaza, H., Quirós, L. M., and Fierro, J. F. (1999) Permeabilizing action of an antimicrobial lactoferricin-derived peptide on bacterial and artificial membranes. *FEBS Lett. 462*, 273−277.

(21) Umeyama, M., Kira, A., Nishimura, K., and Naito, A. (2006) Interactions of bovine lactoferricin with acidic phospholipid bilayers and its antimicrobial activity as studied by solid-state NMR. *Biochim. Biophys. Acta, Biomembr. 1758*, 1523−1528.

(22) Jing, W., Svendsen, J. S., and Vogel, H. J. (2006) Comparison of NMR structures and model-membrane interactions of 15-residue antimicrobial peptides derived from bovine lactoferricin. *Biochem. Cell Biol. 84*, 312−326.

(23) Islam, M. Z., Alam, J. M., Tamba, Y., Karal, M. A. S., and Yamazaki, M. (2014) The single GUV method for revealing the

DOI: 10.1021/acs.biochem.5b00594
Biochemistry 2015, 54, 5802−5814

functions of antimicrobial, pore-forming toxin, and cell-penetrating peptides or proteins. *Phys. Chem. Chem. Phys. 16*, 15752−15767.
(24) Tamba, Y., and Yamazaki, M. (2005) Single giant unilamellar vesicle method reveals effect of antimicrobial peptide, magainin-2, on membrane permeability. *Biochemistry 44*, 15823−15833.
(25) Tamba, Y., and Yamazaki, M. (2009) Magainin 2-induce pore formation in the lipid membranes depends of its concentration in the membrane interface. *J. Phys. Chem. B 113*, 4846−4852.
(26) Tamba, Y., Ariyama, H., Levadny, V., and Yamazaki, M. (2010) Kinetic pathway of antimicrobial peptide magainin 2-induced pore formation in lipid membranes. *J. Phys. Chem. B 114*, 12018−12026.
(27) Karal, M. A. S., Alam, J. M., Takahashi, T., Levadny, V., and Yamazaki, M. (2015) Stretch-Activated Pore of Antimicrobial Peptide Magainin 2. *Langmuir 31*, 3391−3401.
(28) Tamba, Y., Ohba, S., Kubota, M., Yoshioka, H., Yoshioka, H., and Yamazaki, M. (2007) Single GUV method reveals interaction of Tea catechin (−)-epigallocatechin gallate with lipid membranes. *Biophys. J. 92*, 3178−3194.
(29) Schön, P., Garcia-Saez, A. J., Malovrh, P., Bacia, K., Anderluh, G., and Schwille, P. (2008) Equinatoxin II Permeabilizing activity depends on the presence of sphingomyelin and lipid phase coexistence. *Biophys. J. 95*, 691−698.
(30) Fuertes, G., Garcia-Sáez, A., Esteban-Martin, S., Giménez, D., Sánchez-Muñoz, O. L., Schwille, P., and Salgado, J. (2010) Pores formed by Baxα5 relax to a smaller size and keep at equilibrium. *Biophys. J. 99*, 2917−2925.
(31) Apellaniz, B., Nieva, J. L., Schwille, P., and García-Sáez, A. J. (2010) All-or-none versus graded: single-vesicle analysis reveals lipid composition effects on membrane permeabilization. *Biophys. J. 99*, 3619−3628.
(32) Ahmad, A., Azmi, S., Srivastava, R. M., Srivastava, S., Pandey, B. K., Saxena, R., Bajpai, V. K., and Ghosh, J. K. (2009) Design of nontoxic analogues of cathelicidin-derived bovine antimicrobial peptide BMAP-27: the role of leucine as well as phenylalanine zipper sequences in determining its toxicity. *Biochemistry 48*, 10905−10917.
(33) Andrews, J. M. (2001) Determination of minimum inhibitory concentrations. *J. Antimicrob. Chemother. 48* (S1), 5−16.
(34) Bartlett, G. R. (1959) Phosphorous assay in column chromatography. *J. Biol. Chem. 234*, 466−468.
(35) Tamba, Y., Terashima, H., and Yamazaki, M. (2011) A membrane filtering method for the purification of giant unilamellar vesicles. *Chem. Phys. Lipids 164*, 351−358.
(36) Oka, T., Tsuboi, T., Saiki, T., Takahashi, T., Alam, J. M., and Yamazaki, M. (2014) Initial Step of pH-Jump-Induced Lamellar to Bicontinuous Cubic Phase Transition in Dioleoylphosphatidylserine/Monoolein. *Langmuir 30*, 8131−8140.
(37) Roth, B. L., Poot, M., Yue, S. T., and Millard, P. J. (1997) Bacterial viability and antibiotic susceptibility testing with SYTOX green nucleic acid stain. *Appl. Env. Microbiol. 63*, 2421−2431.
(38) Mukherjee, S., Zheng, H., Derebe, M. G., Callenberg, K. M., Partch, C. L., Rollins, D., Propheter, D., Rizo, J., Grabe, M., Jiang, Q.-X., and Hooper, L. V. (2014) Antibacterial membrane attack by a pore-forming intestinal C-type lectin. *Nature 505*, 103−107.
(39) Islam, M. Z., Ariyama, H., Alam, J. M., and Yamazaki, M. (2014) Entry of cell-penetrating peptide transportan 10 into a single vesicle by translocating across lipid membrane and its induced pores. *Biochemistry 53*, 386−396.
(40) Goins, A. B., Sanabria, H., and Waxham, M. N. (2008) Macromolecular crowding and size effects on probe microviscosity. *Biophys. J. 95*, 5362−5373.
(41) Israelachvili, J. N. (1992) *Intermolecular and Surface Forces*, 2nd ed., Academic Press, New York.
(42) McLaughlin, S., and Murray, D. (2005) Plasma membrane phosphoinositide organization by protein electrostatics. *Nature 438*, 605−611.
(43) Karal, M. A. S., Levadnyy, V., Tsuboi, T., Belaya, M., and Yamazaki, M. (2015) Electrostatic interaction effects on tension-induced pore formation in lipid membranes. *Phys. Rev. E 92*, 012708.
(44) Farge, E., and Devaux, P. F. (1992) Shape changes of giant liposomes induced by an asymmetric transmembrane distribution of phospholipids. *Biophys. J. 61*, 347−357.
(45) Tanaka, T., Tamba, Y., Masum, S. M., Yamashita, Y., and Yamazaki, M. (2002) La^{3+} and Gd^{3+} induce shape change of giant unilamellar vesicles of phosphatidylcholine. *Biochim. Biophys. Acta, Biomembr. 1564*, 173−182.
(46) Yamashita, Y., Masum, S. M., Tanaka, T., and Yamazaki, M. (2002) Shape changes of giant unilamellar vesicles of phosphatidylcholine induced by a de novo designed peptide interacting with their membrane interface. *Langmuir 18*, 9638−9641.
(47) Tanaka, T., Sano, R., Yamashita, Y., and Yamazaki, M. (2004) Shape changes and vesicle fission of giant unilamellar vesicles of liquid-ordered phase membrane induced by lysophosphatidylcholine. *Langmuir 20*, 9526−9534.
(48) Lopez-Montero, I., Rodriguez, N., Cribier, S., Pohl, A., Velez, M., and Devaux, P. F. (2005) Rapid transbilayer movement of ceramides in phospholipid vesicles and in human erythrocytes. *J. Biol. Chem. 280*, 25811−25819.
(49) Heinrich, V., Svetina, S., and Zeks, B. (1993) Nonaxisymmetric vesicle shapes in a generalized bilayer- couple model and the transition between oblate and prolate axisymmetric shapes. *Phys. Rev. E: Stat. Phys., Plasmas, Fluids, Relat. Interdiscip. Top. 48*, 3112−3123.
(50) Miao, L., Seifert, U., Wortis, M., and Döbereiner, H.-G. (1994) Budding transitions of fluid-bilayer vesicles: The effect of area-difference elasticity. *Phys. Rev. E: Stat. Phys., Plasmas, Fluids, Relat. Interdiscip. Top. 49*, 5389−5407.
(51) Yamazaki, M., and Ito, T. (1990) Deformation and instability in membrane structure of phospholipid vesicles caused by osmophobic association: Mechanical stress model for the mechanism of poly (ethylene glycol)-induced membrane fusion. *Biochemistry 29*, 1309−1314.
(52) Domingues, T. M., Riske, K. A., and Miranda, A. (2010) Revealing the lytic mechanism of antimicrobial peptide gomesin by observing giant unilamellar vesicles. *Langmuir 26*, 11077−11084.
(53) Evans, E., Heinrich, V., Ludwig, F., and Rawicz, W. (2003) Dynamic tension spectroscopy and strength of biomembranes. *Biophys. J. 85*, 2342−2350.
(54) Evans, E., and Smith, B. A. (2011) Kinetics of hole nucleation in biomembrane rupture. *New J. Phys. 13*, 095010 (29 pages).
(55) Sandre, O., Moreaux, L., and Brochard-Wyart, F. (1999) Dynamics of transient pores in stretched vesicles. *Proc. Natl. Acad. Sci. U. S. A. 96*, 10591−10596.
(56) Karatekin, E., Sandre, O., Guitouni, H., Borghi, N., Puech, P. −H., and Brochard-Wyart, F. (2003) Cascades of transient pores in giant vesicles: line tension and transport. *Biophys. J. 84*, 1734−1749.
(57) Levadny, V., Tsuboi, T., Belaya, M., and Yamazaki, M. (2013) Rate constant of tension-induced pore formation in lipid membranes. *Langmuir 29*, 3848−3852.
(58) Litster, J. D. (1975) Stability of lipid bilayers and red blood cell membranes. *Phys. Lett. A 53*, 193−194.
(59) Taupin, C., Dvolaitzky, M., and Sauterey, C. (1975) Osmotic pressure induced pores in phospholipid vesicles. *Biochemistry 14*, 4771−4775.
(60) Karal, M. A. S., and Yamazaki, M. (2015) Activation energy of tension-induced pore formation in lipid membranes. *J. Chem. Phys. 143*, 081103.
(61) Wimley, W. C., and White, S. H. (1996) Experimentally determined hydrophobicity scale for proteins at membrane interface. *Nat. Struct. Biol. 3*, 842−848.
(62) Schibli, D. J., Epand, R. F., Vogel, H. J., and Epand, R. M. (2002) Tryptophan-rich antimicrobial peptides: comparative properties and membrane interactions. *Biochem. Cell Biol. 80*, 667−677.
(63) Vogel, H. J., Schibli, D. J., Jing, W., Lohmeier-Vogel, E. M., Epand, R. F., and Epand, R. M. (2002) Towards a structure-function analysis of bovine lactoferricin and related tryptophan- and arginine-containing peptides. *Biochem. Cell Biol. 80*, 49−63.
(64) Pouny, Y., Rapaport, D., Mor, A., Nicolas, P., and Shai, Y. (1992) Interaction of antimicrobial dermaseptin and its fluorescently

DOI: 10.1021/acs.biochem.5b00594
Biochemistry 2015, 54, 5802−5814

labeled analogues with phospholipid membranes. *Biochemistry 31*, 12416−12423.
(65) He, J., and Furmanski, P. (1995) Sequence specificity and transcriptional activation in the binding of lactoferrin to DNA. *Nature 373*, 721−724.
(66) Kanyshkova, T. G., Semenov, D. V., Buneva, V. N., and Nevinsky, G. A. (1999) Human milk lactoferrin binds two DNA molecules with different affinities. *FEBS Lett. 451*, 235−237.
(67) Guyton, A. C., and Hall, J. E. (2006) *Textbook of Medical Physiology*, 11th ed., Elsevier Saunders, Philadelphia.
(68) Cevc, G., and Marsh, D. (1987) *Phospholipid Bilayers*; John Wiley and Sons, New York.

DOI: 10.1021/acs.biochem.5b00594
Biochemistry 2015, 54, 5802−5814